A Technique for the Analysis of Discontinuity Induced Behaviour in Piecewise-Smooth Electronic Oscillators

Peter Harte†, Elena Blokhina†, Dimitri Galayko‡ and Orla Feely†

†School of Electrical, Electronic and Communications Engineering, University College Dublin, Dublin, Ireland
‡Sorbonne Universités, UPMC Univ Paris 06, UMR 7606, LIP6, F-75005, Paris, France
Email: peter.harte@ucdconnect.ie, elena.blokhina@ucd.ie, dimitri.galayko@lip6.fr, orla.feely@ucd.ie

Abstract—This paper presents a visualisation technique that facilitates the analysis of the discontinuity induced behaviour that appears in piecewise-smooth electronic oscillators. In this work, an electrostatic vibration energy harvester is the system used to present the new technique.

1. Introduction

In this work we present a technique which aids in the analysis of discontinuity induced behaviour in piecewise-smooth electronic oscillators. The developed technique is used to examine the dynamics of a particular type of piecewise smooth oscillator, namely an electrostatic vibration energy harvester (eVEH). An eVEH is a device that generates electrical energy from ambient vibrations in its surrounding environment by employing a high-quality micro-resonator (linear or nonlinear) and conditioning electronics, coupled together through a variable capacitor (the transducer).

It was shown in [1] that this system displays both regular and irregular behaviour, and it was later confirmed in [2, 3, 4] that both classical nonlinear phenomena and sliding phenomena were present in the system. This nonlinear behaviour appears due to the eVEH being a mixed system i.e. the electro-mechanical coupling of the transducer, along with the switched nature of the conditioning electronics. The switching of the conditioning electronics causes a discontinuity in the vector field describing the system. This explains the appearance of sliding behaviour in the system, an analysis of which can be found in [4]. Sliding behaviour can be particularly detrimental to the performance of an eVEH. This is because the system's switches operate upon the detection of local extrema of a varying capacitance. When sliding occurs, many local maxima and minima of this capacitance also occur, causing many switching events.

In [3] and [4], bifurcation diagrams were presented that allowed one to get an overview of the whole system dynamics of an eVEH. It was apparent from these plots that sliding motion was very much present in the system. The particularities of this sliding behaviour however could not be determined from a bifurcation diagram alone. The motivation behind this paper is to develop a visualisation tool based upon a traditional bifurcation diagram which also highlights the discontinuity induced behaviour present in a piecewise-smooth system like an eVEH. This technique can be extended to any electronic oscillator that displays such sliding phenomena.

2. Statement of the Problem

The piecewise-smooth electronic oscillator used in this work to present our analysis technique, models an eVEH and is shown in Fig. 1. It consists of a high-Q linear or nonlinear resonator, a variable capacitor (transducer) and a conditioning circuit that implements the constant-charge energy conversion cycle [5]. Ambient vibrations of the environment in which the eVEH is situated cause the transducer to oscillate since it is attached to a high-Q linear or nonlinear resonator. This oscillation causes the capacitance of the variable capacitor $C_{\text{tran}}(t)$ to vary with time. The conditioning circuitry discharges C_{tran} to zero at a local minimum of the capacitance and charges C_{tran} to a charge Q_0 at a local maximum. This is done by fixing an energy W_0 on the capacitor at every local maximum. The mechanical-to-electrical energy conversion occurs whilst the transducer capacitance decreases from a local maximum to a local minimum by keeping the charge constant thus increasing the voltage between the plates.

By introducing both a variable vector $\mathbf{x} = (x_1, x_2, x_3)$, where x_1 represents the normalised displacement, x_2 the normalised velocity and x_3 dimensionless time, and a vector representing the system parameters $\mathbf{P} = (\beta, \alpha, \Omega, \nu_{\text{W}})$, the system dynamics of an eVEH can be described by

$$\dot{\mathbf{x}} = \begin{cases} \mathbf{F}_1(\mathbf{x}, \mathbf{P}), & H(\mathbf{x}) > 0 \\ \mathbf{F}_2(\mathbf{x}, \mathbf{P}), & H(\mathbf{x}) < 0 \end{cases} \tag{1}$$

where

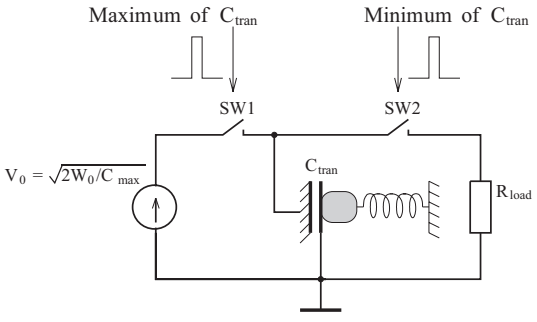

Figure 1: Schematic of the electronic oscillator which models a vibration electrostatic energy harvester.

$$\mathbf{F}_1(\mathbf{x},\mathbf{P}) = \mathbf{F}_2(\mathbf{x},\mathbf{P}) + \begin{bmatrix} 0 \\ \frac{\nu_W}{1-x_{1,\max}} \\ 0 \end{bmatrix} \tag{2}$$

and

$$\mathbf{F}_2(\mathbf{x},\mathbf{P}) = \begin{cases} x_2 \\ -2\beta x_2 - x_1 - \sum_{n=2}^{N} \kappa_n x_1^n + \alpha \cos\,\Omega x_3 \\ 1 \end{cases} \tag{3}$$

This general system (1) can be used to describe an eVEH whether it is operated with a linear or nonlinear resonator. In (1), $x_1 = x/d$, $\beta = b/(2m\omega_0)$, $\kappa_n = \frac{k_n d^{n-1}}{m\omega_0^2}$, $\alpha = A_{ext}/(d\omega_0^2)$, $\nu_W = W_0/(d^2 m\omega_0^2)$, $\Omega = \omega_{ext}/\omega_0 = 1+\sigma$ (σ is a possible small mismatch between the two frequencies) and $x_3 = \omega_0 t$. These are all derived from the dimensional parameters describing the system: displacement x, the transducer gap at rest d, the damping factor b, resonator mass m, the natural frequency of the resonator $\omega_0 = \sqrt{k_1/m}$ (k_1 is the linear spring constant), the mechanical nonlinearity coefficients of a nonlinear resonator $k_n (n \geq 2)$, the energy fixed on the transducer W_0, the acceleration A_{ext} and frequency ω_{ext} of the ambient vibrations, and time t. It is clear to see from (1) that a discontinuity exists in the system. The boundary between the two vector fields governing the system is referred to as the switching surface Σ. The scalar function $H(\mathbf{x})$ that defines Σ is given by the switching condition $H(\mathbf{x}) = -x_2 = 0$. A more detailed description of the mathematical model and operation of this system can be found in [2]. General system parameters used throughout this paper can be seen in Table 1.

Table 1: General parameter values and ranges of the studied eVEH used throughout this paper (unless stated otherwise).

System Parameters	
m	$200 \cdot 10^{-6}$ kg
b	$1.5 \cdot 10^{-3}$ Nsm^{-1}
k_1	300 Nm^{-1}
d	$20{\cdot}10^{-6}$ m
C_0	$44.25 \cdot 10^{-12}$ F
σ	0.03

3. Visualisation of Discontinuity Induced Bifurcations

3.1. Bifurcation Diagrams

Bifurcation diagrams like the one seen in Fig. 2 for an eVEH were presented in [3] and [4]. In the particular instance of Fig. 2, the acceleration of the external vibrations being harnessed, A_{ext}, is varied as all other parameters are held constant. For each point the initial conditions are taken to be $x_1 = 0$ and $x_2 = 0$, and (1) is evaluated for 1500 units of dimensionless time x_3. Any local maxima that occur between $x_3 = 1200$ and $x_3 = 1500$ are plotted. The first 1200 units of x_3 are neglected to ensure that the transient process has passed. It is clear that the bifurcation diagram displays classical nonlinear behaviour e.g. cascades of doubling bifurcations and intermittency. What is not as easily explained is the appearance of these lower branches in the figure at $A_{ext} < 2\text{ms}^{-2}$ and at $A_{ext} > 7\text{ms}^{-2}$. In [4] it was noted that this phenomena is actually discontinuity induced behaviour i.e. sliding motion. This sliding motion appears in a bifurcation diagram because it contains many maxima, since a trajectory undergoing sliding continuously switches between the two subspaces of the system $\mathbf{F}_1$ and $\mathbf{F}_2$.

3.2. Discontinuity Induced Behaviour

Sliding motion or discontinuity induced behaviour can occur in piecewise smooth systems like an eVEH when a trajectory intersects the switching surface Σ through particular regions on the switching manifold known as 'sliding regions' [6]. Since $\mathbf{F}_1$ describes the flow of system (1) when $H(\mathbf{x}) > 0$ and $\mathbf{F}_2$ describes the flow when $H(\mathbf{x}) < 0$ then we can construct $\mathbf{F}_s$, a specific vector field that governs the flow inside the switching region when $H(\mathbf{x}) = 0$, using Utkins equivalent control method [7].

$$\mathbf{F}_s = \frac{\mathbf{F}_1 + \mathbf{F}_2}{2} + \rho(\mathbf{x})\frac{\mathbf{F}_2 - \mathbf{F}_1}{2} \tag{4}$$

where $|\rho| \leq 1$. The normal vector $\mathbf{n}^T = [\nabla H(\mathbf{x})]^T = (0,-1,0)$ is directed towards the subspace governed by the vector field $\mathbf{F}_1$. Using the notation $\langle \mathbf{a}, \mathbf{b} \rangle$ to denote the inner product of two vectors, the function $\rho(\mathbf{x})$ can be obtained by considering that $\mathbf{F}_s$ must be tangential to the switching manifold Σ, which means that $\langle \mathbf{n}^T, \mathbf{F}_s \rangle = 0$. Thus we obtain that

$$\rho(\mathbf{x}) = \frac{\langle \mathbf{n}^T, \mathbf{F}_1 \rangle + \langle \mathbf{n}^T, \mathbf{F}_2 \rangle}{\langle \mathbf{n}^T, \mathbf{F}_1 \rangle - \langle \mathbf{n}^T, \mathbf{F}_2 \rangle} \tag{5}$$

The boundaries of the sliding regions are defined by the corresponding conditions

$$\hat{\Sigma}^+ = \{\mathbf{x} \in \Sigma / \rho(\mathbf{x}) = +1\} \tag{6}$$

and

$$\hat{\Sigma}^- = \{\mathbf{x} \in \Sigma / \rho(\mathbf{x}) = -1\} \tag{7}$$

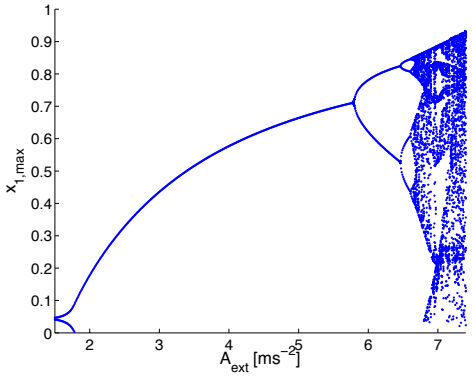

Figure 2: Bifurcation diagram for an eVEH operated with a linear resonator. Local maxima of displacement are plotted as A_{ext} varies while W_0 is fixed at 10 nJ.

These expressions (6) and (7) are used to determine the sliding regions of an eVEH since a sliding region is bounded by $\hat{\Sigma}^+$ and $\hat{\Sigma}^-$. Evaluating (6) and (7) for an eVEH operating in constant-charge mode we obtain the following expressions for the $\hat{\Sigma}^+$ and $\hat{\Sigma}^-$ boundaries

$$\hat{\Sigma}^+ : \; x_1 + \sum_{n=2}^{N} \kappa_n \, x_1^n - \alpha \cos \, \Omega x_3 = 0 \qquad (8)$$

and

$$\hat{\Sigma}^- : \; x_1 + \sum_{n=2}^{N} \kappa_n \, x_1^n - \alpha \cos \, \Omega x_3 - \frac{\nu_W}{1 - x_1} = 0 \qquad (9)$$

The expressions (8) and (9) define the boundaries of the sliding regions on the switching surface $H(\mathbf{x}) = 0$. If a trajectory crosses the switching surface through one of these sliding regions then sliding motion will occur. The trajectory will cross Σ transversely until it hits one of the boundaries of the sliding region. These sliding region boundaries (8) and (9) change and evolve depending upon system parameter values and thus the sliding regions themselves evolve [4].

3.3. Sliding Bifurcation Diagrams

The simulations that were used to find the results in Fig. 2 were repeated but this time the values for x_3 corresponding to each detection of a maximum of displacement were also recorded. Using these times in conjunction with (8) and (9) it can be determined whether a particular segment of a trajectory contains sliding motion or not, and if so, then by which boundary $\hat{\Sigma}^+$ or $\hat{\Sigma}^-$, this segment leaves the sliding region.

In Fig. 3 (a) one can see the results of this process for an eVEH operated with a linear resonator and $W_0 = 10$nJ. With this visualisation tool, the blue dots correspond to local maxima from a segment of a trajectory that crosses the discontinuity boundary outside the sliding regions. The pink and green points correspond to local maxima that appear due to sliding. The green points indicate that the sliding segment of the trajectory leaves the sliding region through the $\hat{\Sigma}^+$ boundary and the pink points indicate that the sliding segment of the trajectory leaves the sliding region through the $\hat{\Sigma}^-$ boundary. These mappings can also be written as

$$\mathcal{D} = \left\{ (x_1, x_2, x_3) \in \mathcal{R}^3 / H(\mathbf{x}) = 0, \; \frac{dx_2}{dx_3} < 0 \right\} \qquad (10)$$

$$\mathcal{D}_\Sigma^+ = \left\{ (x_1, x_2, x_3) \in \mathcal{R}^3 / \rho(\mathbf{x}) = +1 \right\} \qquad (11)$$

$$\mathcal{D}_\Sigma^- = \left\{ (x_1, x_2, x_3) \in \mathcal{R}^3 / \rho(\mathbf{x}) = -1 \right\} \qquad (12)$$

where (10) corresponds to the blue points, (11) to the green points and (12) to the pink points.

Comparing Fig. 2 and Fig. 3 (a) it is clear that it is now much easier to quickly determine where the sliding motion appears in the system. Sliding motion appears and disappears in a system by discontinuity induced bifurcations

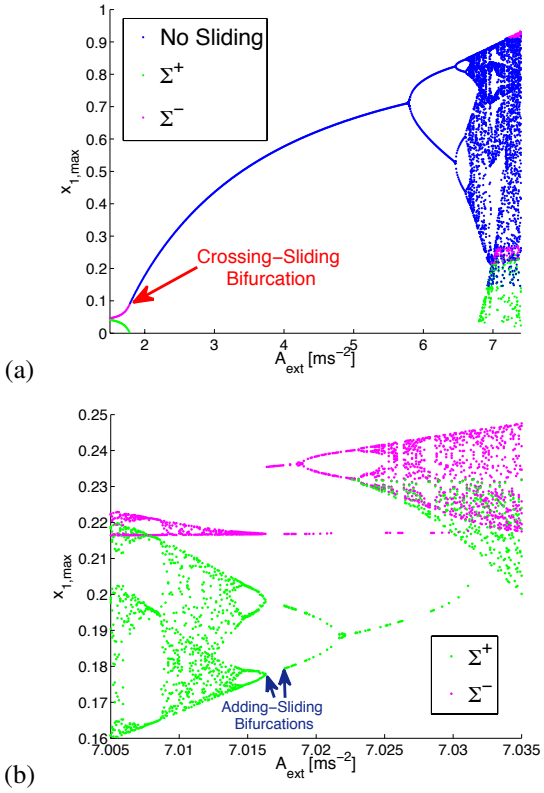

Figure 3: Sliding bifurcation diagram. (a): $W_0 = 10$nJ, linear resonator. (b): Magnified section of (a), omitting non-sliding points.

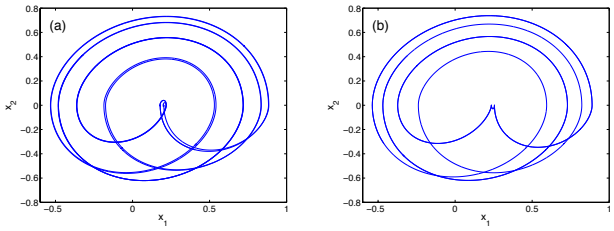

Figure 4: Effect of adding-sliding bifurcation on phase of system. (a) $A_{ext} = 7.0163$ms^{-2}: 10T-orbit. (b) $A_{ext} = 7.0164$ms^{-2}: 5T-orbit. Note the disappearance of a loop due to the adding-sliding bifurcation.

(sliding bifurcations) [6]. These sliding bifurcations are so called since they cause a qualitative change in a system's orbit. The visualisation technique presented here aids us in determining firstly, when these sliding bifurcations occur in a system and secondly, what types of sliding bifurcations occur. It was shown in [4] that there are two types of sliding bifurcations that can occur in an eVEH: a crossing-sliding bifurcation and an adding-sliding bifurcation.

Looking at Fig. 3 (a) we can see that the sliding that is present at low values of A_{ext} completely disappears from $A_{ext} = 1.78$ms^{-2} to $A_{ext} = 1.79$ms^{-2}. This happens due to a crossing-sliding bifurcation. Some of the sliding motion

that exists at higher values of A_{ext} can be seen in more detail in Fig. 3 (b) where the points mapped by (10) have been omitted to ease the analysis of the sliding regimes. Two adding-sliding bifurcations are marked on the figure. The first occurs at $A_{ext} \approx 7.01635\text{ms}^{-2}$. One can observe how the green points representing contact with the $\hat{\Sigma}^+$ boundary disappear, and all that remains is a single pink point. This adding-sliding bifurcation creates a window of periodicity with a segment of sliding motion. This window disappears again via another adding-sliding bifurcation at $A_{ext} \approx 7.01765\text{ms}^{-2}$. The effect that an adding-sliding can have on the phase of this system can be seen in Fig. 4. In Fig. 4 (a) one can see a 10T-orbit before the adding-sliding bifurcation and in Fig. 4 (b) a 5T-orbit (a loop of which has disappeared) after the adding-sliding bifurcation.

Fig. 5 (a) shows the dynamics of an eVEH, operated with a nonlinear resonator ($\kappa_3 = 0.3$) and W_0 fixed at 20 nJ , plotted using this new visualisation technique. Again, through the colour coding, one can easily observe at which values of A_{ext} sliding does, and does not, occur. A crossing-sliding bifurcation similar to the one discussed previously occurs between $A_{ext} = 4.05\text{ms}^{-2}$ to $A_{ext} = 4.06\text{ms}^{-2}$. By zooming in on the system's dynamics at higher values of A_{ext} in Fig. 5 (b), it can be seen how the green points 'collide' with the pink points at $A_{ext} = 10.092\text{ms}^{-2}$. This results in a disappearance of the green points. This discontinuity induced behaviour is once again caused by an adding-sliding bifurcation.

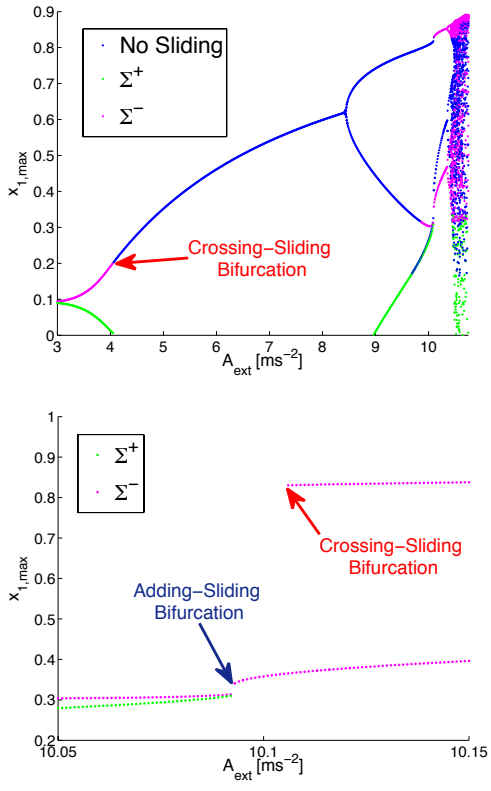

Figure 5: Sliding bifurcation diagram. (a): $W_0 = 20\text{nJ}$, nonlinear resonator ($\kappa_3 = 0.3$). (b): Magnified section of (a), omitting non-sliding points.

4. Conclusions

Discontinuity induced behaviour is a characteristic of piecewise-smooth electronic oscillators. In this work we have presented a visualisation tool that highlights where this discontinuity induced behaviour occurs in a system's dynamics and at the same time facilitates in determining what type of discontinuity induced bifurcation causes this sliding motion to appear or disappear. An electrostatic vibration energy harvester was the system used to present the visualisation technique in this work but the technique can be used to analyse any piecewise-smooth oscillator.

Acknowledgements

The authors would like to thank NOLTA2014 organizing committee members for their fruitful suggestions and comments. This work was funded under the Programme for Research in Third-Level Institutions and co-funded under the European Regional Development Fund.

References

[1] D. Galayko and P. Basset, "A general analytical tool for the design of vibration energy harvesters (VEHs) based on the mechanical impedance concept," *IEEE Trans. Circuits Syst. I*, no. 99, pp. 299–311, 2011.

[2] E. Blokhina, D. Galayko, P. Basset, and O. Feely, "Steady-state oscillations in resonant electrostatic vibration energy harvesters," *IEEE Trans. Circuits Syst. I*, vol. 60, pp. 875 – 884, 2013.

[3] E. O'Riordan, P. Harte, E. Blokhina, D. Galayko, and O. Feely, "Bifurcation scenarios in electrostatic vibration energy harvesters," in *Proc. of the 2012 International Conference on Nonlinear Dynamics of Electronic Systems*, 11–13 July 2012, Wolfenbuttel, Germany, 2012, pp. 34–37.

[4] P. Harte, E. Blokhina, D. Fournier-Prunaret, D. Galayko, and O. Feely, "Electrostatic vibration energy harvesters with linear and nonlinear resonators," *International Journal of Bifurcation and Chaos*, 2014 (In press).

[5] S. Meninger, J. Mur-Miranda, R. Amirtharajah, A. Chandrakasan, and J. Lang, "Vibration-to-electric energy conversion," *Very Large Scale Integration (VLSI) Systems, IEEE Transactions on*, vol. 9, no. 1, pp. 64–76, 2001.

[6] M. Di Bernardo, C. J. Budd, A. R. Champneys, and P. Kowalczyk, *Piecewise-Smooth Dynamical Systems: Theory and Applications*. Springer-Verlag, 2008.

[7] V. Utkin, *Sliding Modes in Control Optimization*. Springer, 1992.